

The metamorphic history of Monte Mucrone metagranodiorite constrained by garnet growth modelling

MARCO BRUNO* and MARCO RUBBO

Dipartimento di Scienze Mineralogiche e Petrologiche, Via Valperga Caluso, 35, I-10125 Torino, Italy

Submitted, November 2005 - Accepted, February 2006

ABSTRACT. — In this work we reconstruct the compositional zoning of the coronitic garnet developed between biotite and plagioclase in the Monte Mucrone metagranodiorite (Sesia Zone, Western Italian Alps) during the HP Alpine metamorphism, by using a modified segregation-dissolution model and supposing slow plagioclase resorption. Information on the rates of burial and exhumation of the rock (0.75 cm/year), on the garnet growth rate ($\sim 9 \times 10^{-17}$ cm/s) and on the evolution of the composition of the minerals (biotite, phengite, plagioclase, K-feldspar, Na-pyroxene) associated to the garnet, have been obtained. Furthermore, we have estimated that the minimum peak pressure recorded by the Monte Mucrone metagranodiorite is 16 kbar.

RIASSUNTO. — In questo lavoro ricostruiamo la zonatura composizionale del granato coronitico sviluppatosi al contatto biotite-plagioclasio nella metagranodiorite del Monte Mucrone (Zona Sesia, Alpi Occidentali, Italia) durante il metamorfismo alpino di alta pressione, usando un modello modificato di segregazione-dissoluzione e supponendo un lento riassorbimento del plagioclasio. L'applicazione del modello di crescita ci ha permesso di stimare la velocità di subduzione e risalita della roccia (0,75 cm/anno), la velocità di crescita del granato ($\sim 9 \times 10^{-17}$ cm/s) e l'evoluzione della composizione dei minerali (biotite, fengite, plagioclasio, K-feldspato, pirosseno

sodico) associati al granato. Inoltre, abbiamo stimato che il picco barico registrato dalla roccia non può essere inferiore a 16 kbar.

KEY WORDS: *Garnet-growth model, partial equilibrium, coronitic garnet, western Alps.*

INTRODUCTION

It has long been demonstrated that chemical zoning in garnet is particularly suitable to extract information on the metamorphic history of the rock. At this end some growth models of garnet consider only its segregation from an equilibrating bulk composition (EBC), rock volume from which the garnet grows, as discussed by Stüwe (1997) and Marmo *et al.* (2002); this is possible when the volume diffusion is sufficiently slow during and after mineral crystallization (e. g., Loomis, 1983; Selverstone *et al.*, 1984; Selverstone and Spear, 1985; Spear and Rumble, 1986; Onge, 1987; Spear, 1988a; Kohn *et al.*, 1992). Since the volume diffusion is capable of relaxing the compositional zoning in garnet at temperatures reached during amphibolite facies metamorphism (e. g., Tracy *et al.*, 1976; Anderson and Olimpio, 1977; Yardley, 1977; Woodsworth, 1977; Loomis, 1978a, 1978b; Dempster, 1985; Chakraborty and Ganguly, 1991), some models also take into account this aspect

* Corresponding author, E-mail: marco.bruno@unito.it

(Spear, 1988b; Florence and Spear, 1991, 1993; Spear *et al.*, 1991; Lang, 1996; Okudaira, 1996; Carlson, 2002). An extensive review of works on diffusion and growth zoning can be found in Spear (1993).

To explain the main features of the chemical zoning of the coronitic garnet developed between biotite and plagioclase in the Monte Mucrone metagranodiorite (MMM), from the Sesia Zone, Western Italian Alps, Rubbo *et al.* (1999) have proposed to modify the EBC not only by the segregation of the garnet, but also by the dissolution of plagioclase, which is known to be slow (Loomis, 1981). The role of plagioclase in determining the garnet composition was also recognized by Spear *et al.* (1991).

The zoning calculated by Rubbo *et al.* (1999) does not fit satisfactory the composition of the garnet rim because the internal re-equilibration of garnet is neglected: it can be acceptable at low temperatures, but not close to the thermal peak. In this paper we start from the work of Rubbo *et al.* (1999), but we also consider diffusion in garnet. Thus, with an iterative procedure, similar to that of Florence and Spear (1991), the thin layers of garnet grown at T , P and time t are slightly perturbed by diffusion over a time interval δt , before calculating the reactions at $T + \delta T$, $P + \delta P$.

It will be shown that strong compositional gradients promoted volume diffusion in garnet, that the garnet experienced partial dissolution during the retrograde path and that the composition of the remaining garnet is a record of its whole history.

In the last part of the work we will discuss critically our results and stress the potential utility of this simulation.

GEOLOGY AND PETROGRAPHY

The MMM crops out in the "Eclogitic Micaschist Complex" (EMC), which is one of the main subunits making up the Sesia Zone (Dal Piaz *et al.*, 1972; Compagnoni and Maffeo, 1973; Compagnoni, 1977; Compagnoni *et al.*, 1977; Koons *et al.*, 1987; Zucali *et al.*, 2002). The Sesia Zone is characterized by the widespread occurrence of eclogites in a wide spectrum of continental crustal lithologies. The EMC of the Sesia Zone is a fragment of Variscan continental

crust, which was metamorphosed during the early Alpine HP subduction event (Oberhänsli *et al.*, 1985; Rubatto *et al.*, 1999). The early Alpine HP stage is constrained at $T=500-600$ °C and $P=13-20$ kbar (Compagnoni, 1977; Koons, 1982; Lardeaux *et al.*, 1982; Droop *et al.*, 1990; Tropper and Essene, 2002) and it has been recently dated at 60-70 Ma by Inger *et al.* (1996), 69.2 ± 2.7 Ma by Duchêne *et al.* (1997), and ~ 65 Ma by Rubatto *et al.* (1999).

The original igneous microstructure of the granodiorite was preserved owing to the absence of pervasive Alpine deformation, and so metamorphic recrystallization was limited to the development of pseudomorphs and coronas at the expense of the original assemblage of quartz, plagioclase, K-feldspar, biotite and accessories. During the HP metamorphism plagioclase was replaced by the assemblage Zo+Jd+Qtz+Kfs (abbreviations follow Kretz, 1983), and at the same time, coronitic garnet developed between biotite and adjacent minerals. Where the biotite was in contact with igneous plagioclase, a composite corona developed (Fig. 1a), consisting of an inner moat of phengite I (Ph I) followed by a moat of garnet and by an outer moat composed of quartz + phengite II (Ph II) intergrowth (Fig. 1b). A more detailed description of the rock and representative analyses of the phases are reported in Rubbo *et al.* (1999); for the sake of brevity we will concentrate on garnet.

Garnet analyses were performed, with a LINK-EDS equipped, Cambridge SEM, at the Dipartimento di Scienze Mineralogiche e Petrologiche, Università di Torino. Natural silicates and oxides were used as standards; accelerating voltage was 15 kV, the integration time 35 s and ZAF data reduction was used. The garnet is mainly an almandine-pyrope-grossular solid solution (Fig. 2a). The Fe and the Ca decreases and increases, respectively, from biotite to phengite II. Towards the garnet/biotite interface, the gradient of grossular molar fraction is less steep than towards the garnet/phengite II interface.

Compositional X-ray maps (Rubbo *et al.*, 1999) show closed iso-concentration patterns indicating that the corona resulted from the coalescence of single garnet crystals; the slab of about $60 \mu\text{m} \times 500 \mu\text{m}$, enlarged in Fig. 1b, is indeed a polycrystalline aggregate. We have analyzed garnet sections of a relatively high area, which should correspond to

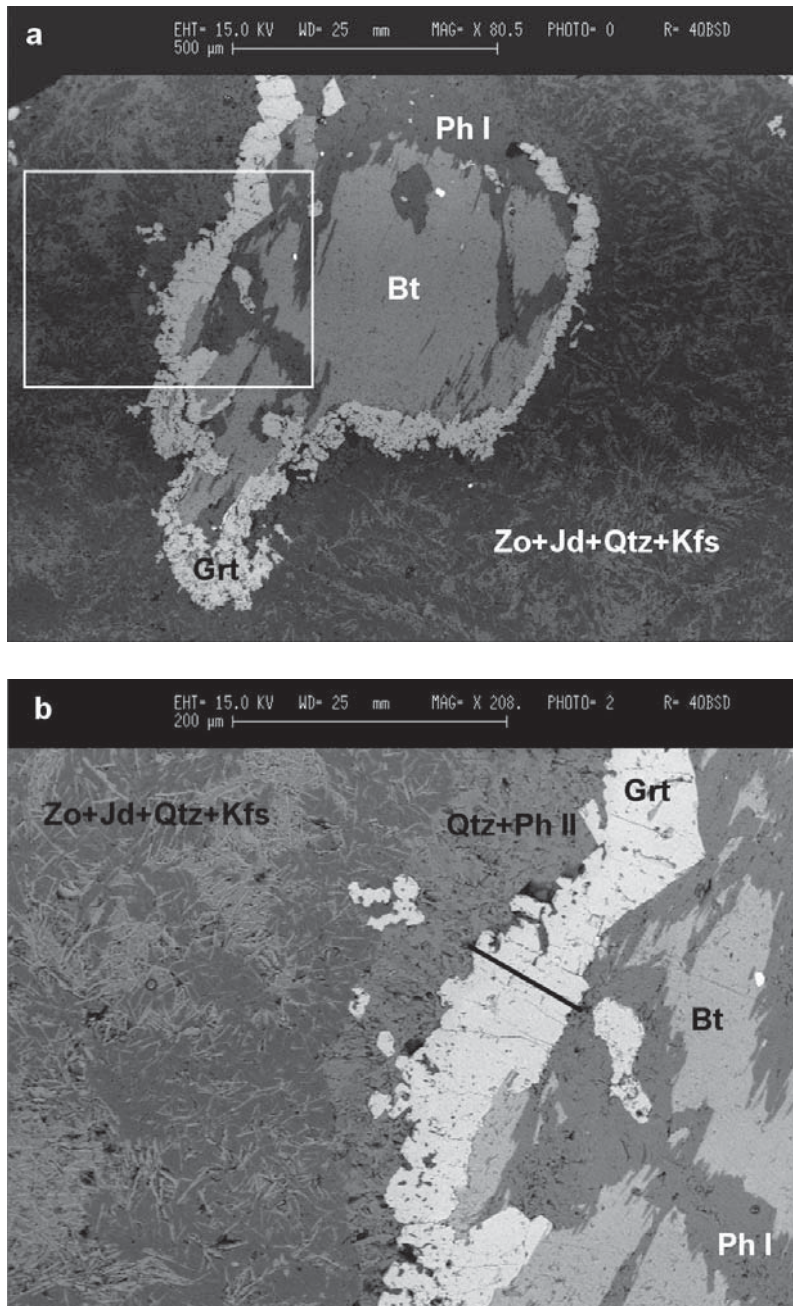


Fig. 1 – SEM backscattered images of the Monte Mucrone metagranodiorite. (a) Biotite included in plagioclase. Presently the plagioclase is totally replaced by Zo+Jd+Qtz+Kfs aggregates, biotite is partially replaced by phengite, and a garnet corona developed between biotite and plagioclase. (b) Region enclosed in the white square in (a); the measurements of Fig. 2a were made along the black line across the garnet corona.

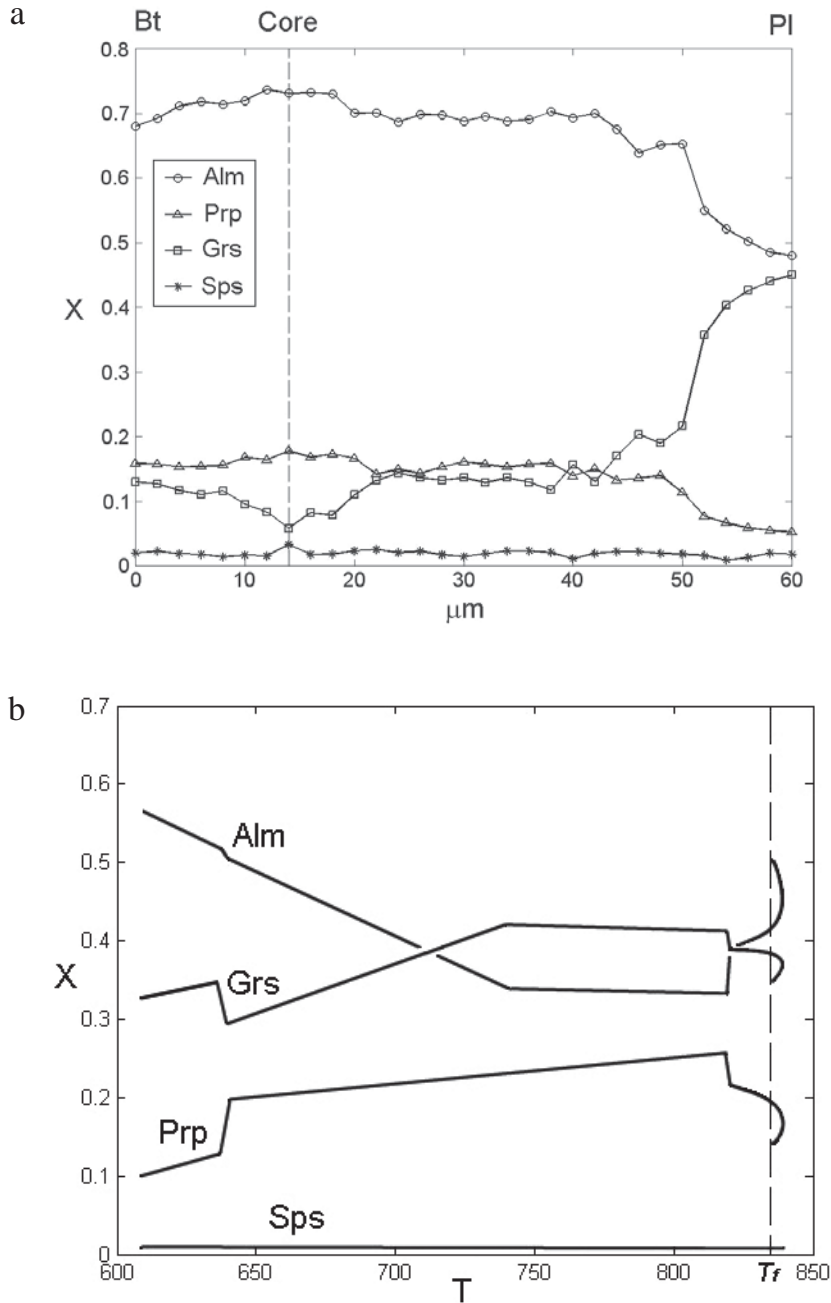


Fig. 2 – (a) Quantitative composition (X, molar fraction) profile across the garnet corona of Fig. 1b. Bt, Core and PI indicate the biotite/garnet interface, the garnet core and the garnet/plagioclase interface, respectively. (b) Equilibrium garnet composition calculated along the P - T path of Fig. 3. T_f is the temperature corresponding to the point c in Fig. 3. When T is greater than T_f , two values of pressure correspond at each temperature, and by consequence, two values of garnet composition.

garnets cut close to their equatorial plane (Fig. 1b). A typical composition is plotted in Fig. 2a. These sections can be recognized from the widest variation of grossular mole fraction from core to rim and from the lowest concentration of grossular in the garnet core. We show that at the lowest temperature and pressure at which garnet could form, the concentration of grossular in the garnet core was the consequence of a non equilibrium process. Indeed, let compare the measured garnet composition (Fig. 2a) with the equilibrium one (Fig. 2b) we have calculated¹ along the P - T path shown in Fig. 3, which is the trajectory estimated in this work for the MMM by reproducing the chemical garnet zoning with the growth model described in the following. The differences between the diagrams of Fig. 2a and Fig. 2b are striking, and as we want to show, at the lowest temperature and pressure values, the concentration of Ca in garnet, when equilibrium prevails, should be much higher than the measured one. This comparison not only helps identifying the garnet core but also it is an indication that the garnet nuclei formed in a Ca-poor environment for two possible causes: a) the sluggishness of the plagioclase reaction and of the intergranular rate of diffusion of its components as discussed in Rubbo *et al.* (1999), and b) the low concentration of Ca in the plagioclase rim.

In order to rationalize the asymmetry of the garnets zoning we present the following qualitative arguments. The shape of crystals was dictated by the surface energy at the time of nucleation, and subsequently by the anisotropy of both the growth rates and the incoming fluxes of components. Because of the high symmetry of the garnet and the absence of strain, we suppose that initially the garnet had a highly isotropic shape. It is likely that during the first growth stages, the diffusion field around every garnet making the corona was spherical. With increasing temperature and pressure the spherical symmetry of shape and composition, was progressively destroyed for the overlapping of the diffusion fields around each crystal, for the coalescence of garnets and, consequently, for the uneven concentration of elements (in particular Mg, Fe, Mn, Ca), diffusing from biotite and from

plagioclase, towards opposite sides of the garnets building the corona. As a consequence the garnets not only exhibit an asymmetric zoning but also grew more quickly towards the plagioclase.

To simplify this very complex problem of reaction and diffusion, we modelled the growth of spherical garnets in a symmetrical diffusion field. However, others garnet shapes have also been tested, as we will refer in a later section.

Finally, the zoning calculated from the garnet core to the face towards plagioclase, will be compared with the measured one.

MODEL DESCRIPTION

To reconstruct the garnet evolution we propose a modified segregation-dissolution model, that can be best described recalling the simulation steps. The iterative calculations start at given initial values of temperature (T_i), pressure (P_i) and amounts of phases determining the initial EBC. The EBC is the bulk composition of the rock's volume which, at given P and T , reacts to produce the equilibrium mineral assemblage (e. g., Stüwe, 1997).

Time, temperature and pressure are iteratively changed by small increments δt , δT and δP , along a P - T trajectory, which has been initially taken from Rubbo *et al.* (1999) and then optimized (reported in Fig. 3) by trial and error to improve the concordance between calculated and measured garnet zoning.

The initial EBC progressively changes with increasing temperature and pressure because of both non-equilibrium growth and dissolution respectively of garnet and plagioclase. When garnet grows its components are subtracted from the EBC, while the components of dissolving plagioclase are added to the EBC.

The amounts grown or dissolved are computed according to Eq. (1).

$$M_\varphi = E_\varphi(T_k, P_k, \mathbf{n}_k) - N_\varphi(T_k - \delta T, P_k - \delta P) \quad (1)$$

M_φ is calculated at every iteration along the P - T - t path. E_φ is the equilibrium number of moles

¹ The bulk composition used in this calculation is reported in Table 1. The phases considered in the equilibrium calculations are: biotite, K-feldspar, plagioclase, quartz, phengite, garnet, Na-pyroxene, zoisite and fluid (H₂O). Details on thermodynamic calculations are reported in the following paragraphs and in Appendix A.

of phase φ (having the equilibrium proportion of end-members) at temperature T_k , pressure P_k and time t_k . It is calculated by minimizing the Gibbs function at the instantaneous EBC. The details of the equilibrium calculations are reported in Appendix A.

N_φ is an empirical Arrhenius type function calculated according to Eqs. (2) and (3).

The growth/dissolution of the phase φ ($\varphi = p$ plagioclase, $\varphi = g$ garnet) is determined by the relative weight of E_φ and N_φ : if the balance (1) is positive, M_φ moles are added to phase φ and subtracted from the EBC; whereas if M_φ is negative, M_φ moles of phase φ are resorbed and added to the EBC.

The expressions of the N_φ are:

$$N_p = \alpha^p \exp\left(\frac{\beta^p}{T_k}\right) \quad (2)$$

$$N_g = \alpha^g \exp\left[\frac{\beta^g (T_k - A)}{T_k}\right] \quad (3)$$

We justify the use of Arrhenius type functions for the N_φ by considering that they are associated to kinetic processes. Indeed, we suppose the Ca abundance in the EBC is determined by two sluggish kinetic processes:

- i) the plagioclase dissolution (Loomis, 1981);
- ii) the intercrystalline diffusion of Ca along grain boundaries. Such assumption is supported by many evidences. In fact, partial equilibrium (meaning disequilibrium for some elements, but not for others) is a common phenomenon during metamorphic mineral growth. Different elements equilibrate over different geologically significant scales of time and length, because they are subject to different rates of intergranular diffusion (e. g., Chernoff and Carlson, 1997; Spear and Daniel, 2001; Carlson, 2002; Hirsch *et al.*, 2003; Konrad-Schmolke *et al.*, 2005). In particular, there are evidences that the Ca fails to equilibrate by intergranular diffusion at temperature below those of the upper amphibolite facies (e. g., Chernoff and Carlson, 1997; Carlson, 2002).

We model these two processes using Eqs. (1)-(3); at this end α^p and β^p in Eq. (2) are chosen to make N_p increasing with temperature. In this way the dissolution of plagioclase increases (and accordingly its input in the EBC) with increasing temperature and by consequence, the Ca increases along the prograde path; α^g, β^g and A make N_g decreasing with temperature, to account for the increase of garnet growth with increasing temperature. However, because the kinetics of reaction and diffusion are slow, the garnet is supposed to grow of a lesser amount than that requested by the equilibrium at T_k, P_k ²: this situation is modeled by Eq. (1) where M_g is generally less than E_g . In some intervals of temperature and pressure M_g is less than zero: this happens when zoisite competes for Ca with garnet, or during retrogression when partial dissolution of garnet occurs.

As it regards the composition, when the garnet grows, the segregated layer is in partitioning equilibrium with the other phases, although its amount (M_g) is less by N_g than that required at equilibrium (E_g); when garnet partially dissolves, its surface is not in partitioning equilibrium with the other phases.

When the balance (1) is positive for garnet, the total amount segregated, M_g , can be distributed: i) in concentric shells, to simulate the growth of a spherical crystal or ii) in parallel slabs to simulate, the advancing of a planar front³. The two cases are an approximation to the really complex garnets growth: we show that the first one works better. In both i) and ii) instances, M_g is distributed around a number of crystals suitable to reproduce the size of the single crystals we measured, as typified in Fig. 2a. Conversely, if it occurs that the balance (1) is negative for garnet at some T_k , and P_k , the inner shells or slabs are resorbed and an amount of components corresponding to M_g moles, is added to the EBC.

It is important to underline that if the function N_g is set to zero the calculation strategy is equivalent to that of Florence and Spear (1991), where all moles of garnet produced over any interval δT and

² The assumption underlying the segregation model is that the intergranular diffusion of components towards the growing phase is not a rate limiting process and that the phase does not dissolve. We relaxed this assumption.

³ The results we present and discuss refer to spherical crystals; for a comparison, the growth of a constant area, planar front, is discussed in the last session.

TABLE 1
Initial moles of biotite, K-feldspar, plagioclase and quartz,
used for the calculations of garnet zoning in the simulation

	Bt				Kfs			Pl		Qtz	
	Ann	Phl	East	Mn-bt	Ab	Or	An	Ab	Or	An	
moles	0.090	0.074	0.086	0.001	0.150	0.600	0.017	1.120	0.080	0.350	0.500

δP are subtracted from the EBC. Our approach is however more general.

Initial values of the parameters α^p , α^s , β^p , β^s and A are from Rubbo *et al.* (1999), because they fit well the low temperature low pressure portion of the garnet zoning. The values are improved by trial and error until the calculated concentrations reproduce satisfactorily also the garnet composition near the rim. The optimal values of the parameters on which N_p and N_g depend, are given in Table 2.

We are aware that our Eqs. (2) and (3) are a crude approximation of the real kinetics and subjected to uncertainty, as we will discuss. Nevertheless this simulation gives a reasonable estimate of the duration of the metamorphic event and we are confident that it is grasping the relevant features of the granodiorite metamorphism.

After deposition/resorption of a garnet layer at T_k , P_k , the volume diffusion in garnet is calculated over a constant time interval δt (re-equilibration time) associated to the increment of pressure and temperature. The cumulative diffusion time represents the duration of the metamorphic event.

We applied Neumann boundary conditions to the diffusion equation⁴, setting zero flow at the garnet surface. The elements diffusing are Ca, Mg, Fe, Mn. The self-diffusion coefficients of these elements are cast in the form of Arrhenius relation:

$$D = D^\circ \exp\left(\frac{-\Delta E - \Delta VP}{RT}\right) \quad (4)$$

where D° is the pre-exponential factor, ΔE is the activation energy at 1 bar, ΔV is the activation volume, P is the pressure, T is the temperature and R is the universal gas constant. To study the

multicomponent diffusion (e. g., Chakraborty and Ganguly, 1991), we use Eq. 5 by Lasaga (1979) to calculate from the self-diffusion coefficients the interdiffusion coefficients (D_{ij}) forming the **D** matrix:

$$D_{ij} = D_i^0 \delta_{ij} - \frac{D_i^0 z_i z_j X_i}{\sum_{k=1}^n z_k^2 X_k D_k^0} (D_j^0 - D_n^0) \quad (5)$$

where δ_{ij} is the Kronecker delta ($i = j$, $\delta_{ij} = 1$; $i \neq j$, $\delta_{ij} = 0$), D_i^0 is the self-diffusion coefficient of the component i , z_i is the charge on the ion i , X_i is the mole fraction of component i ; the n^{th} component is treated as dependent. From Eq. 5 a compositional dependence of the interdiffusion coefficients results, so, the diffusion equation is:

$$\frac{\partial \mathbf{C}}{\partial t} = \frac{1}{r^m} \frac{\partial}{\partial r} \left(r^m \mathbf{D} \frac{\partial \mathbf{C}}{\partial r} \right) \quad (6)$$

where **C** is the (3×1) column vector of the concentrations of Fe, Mg and Ca expressed in mole

TABLE 2
Parameters of the empirical functions, N_p and N_g ,
used to calculate the number of moles of plagioclase
and garnet resorbed at T_k , in the simulation

	α	β	A
Grt	0.041	-12.4	638.7358
Pl	2.700	-5200	-

⁴ In the section "Discussion", calculations performed with different boundary conditions are presented.

fraction, \mathbf{D} is a (3×3) matrix of the interdiffusion coefficients and r the space coordinate. $m = 0$ for cartesian coordinates (planar growth front) and $m = 2$ for spherical coordinates (spherical crystal). The Mn is considered the dependent component. The multicomponent diffusion equation (Eq. 6) is numerically solved.

The sequence of calculation is implemented in a Fortran program (GARGROW), developed by Bruno (2002a, b), integrating the previous routines from Rubbo *et al.* (1999). Switching on or off several routines, one can choose whether or not to consider the volume diffusion in garnet when modeling the zoning.

MODEL APPLICATION

In this section we describe the simulation of the growth of the assembly of garnets between biotite and plagioclase (Fig. 1).

The calculations are performed along the P - T path defined by the Eqs. (7)-(9) and shown in Fig. 3.

$$T_k = A - B \cos(\vartheta + \nu) \quad (7)$$

$$P_k = C - D \cos(\vartheta + \mu) \quad (8)$$

where ϑ is defined as:

$$\vartheta = (k - 1) \frac{\pi}{E} \quad 1 \leq k \leq s; k, s \text{ integers} \quad (9)$$

s is the total number of iterations (number of P and T variations); T_k and P_k are, respectively, the values of temperature (K) and pressure (kbar) at iteration k . A, B, C, D, E, μ and ν are parameters ($A=638.7358$ K; $B=200.5089$; $C=5.340046$ kbar; $D=10.7496704$; $E=15000$; $\mu=2.037473$; $\nu=1.42$) obtained starting from the values by Rubbo *et al.* (1999) and optimized by trial and error, to improve

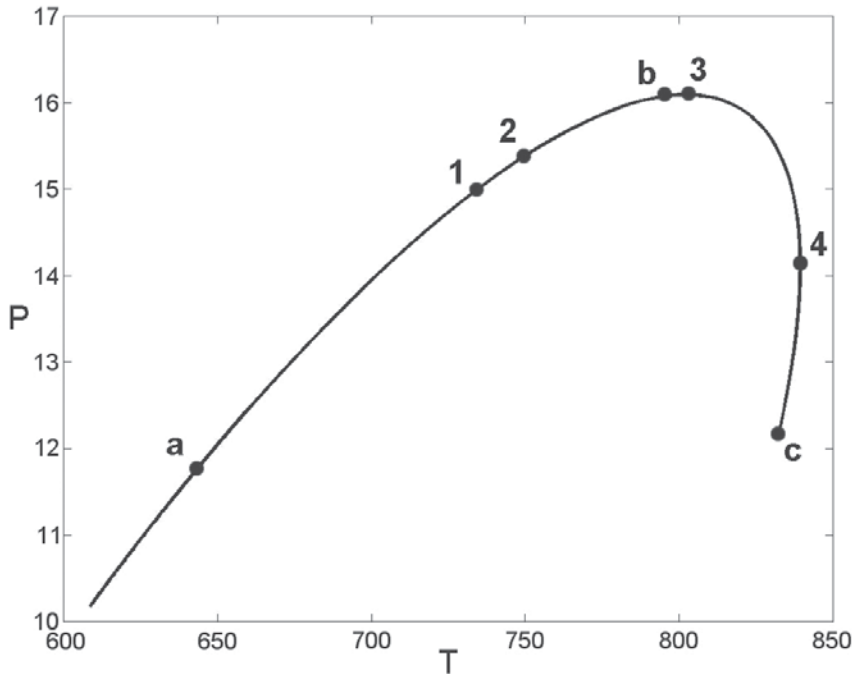


Fig. 3 – P - T paths (P in kbar, T in K) considered in the garnet growth simulation; **a**, **b** and **c** indicate, respectively, where the garnet appears, where the garnet has the maximum radius and where the simulation stops. **1**, **2**, **3** and **4** indicate the P - T conditions of the garnet zonings reported in Fig. 6. In particular, **3** is the pressure peak ($P=16.09$ kbar, $T=802$ K) and **4** the thermal peak ($T=839$ K, $P=14.11$ kbar).

the concordance between calculated and measured garnet zoning.

The initial EBC, reported in Table 1, is calculated considering the system composed by the igneous phases biotite, K-feldspar, plagioclase, and quartz; their composition is typical of the minerals of the granodiorites. The plagioclase is progressively added to the EBC, as prescribed by Eqs. (1) and (2).

In the thermodynamic calculation, in addition to the mentioned phases, we consider phengite, garnet, Na-pyroxene, zoisite, corresponding to the phases observed in the metagranodiorite. The phase components considered are: annite, phlogopite, eastonite and Mn-biotite for biotite; albite, anorthite and orthoclase for feldspars; muscovite, Fe-celadonite and Mg-celadonite for potassic white mica; almandine, grossular, pyrope and spessartine for garnet; jadeite and Ca-Tschemak for Na-pyroxene. We included in the calculation a fluid, supposed to be pure H₂O, setting its initial amount to zero⁵.

With respect to the work by Rubbo *et al.* (1999), the end-member Ca-Tschemak has been included and a more calcic K-feldspar is considered and the amount of biotite has been reduced to a half; the initial EBC has been modified to obtain an increase of the Ca content in the garnet with respect to the simulations performed by Rubbo *et al.* (1999).

The thermodynamic properties are taken from the Holland and Powell (1990) database, updated by Vance and Holland (1993). The solid solution models for biotite and phengite are from Powell (1978), Holland and Powell (1990) and Vance and Holland (1993); for garnet from Ganguly *et al.* (1996); for feldspars from Fuhrman and Lindsley (1988); and for Na-pyroxene a simple molecular mixing is considered.

The kinetics parameters describing the volume diffusion in garnet are reported in Table 3; they have been initially taken from Chakraborty and Ganguly (1992) and Ganguly *et al.* (1998), and then slightly modified to improve the similarity between measured and calculated zoning.

The P - T - t trajectory is covered in 4907 steps δP , δT and associated time δt . The time step δt was progressively decreased to a limiting value that did not produce a significant variation of the zoning calculated. The estimates of the duration of the metamorphic events are not a priori constrained, but they are an output of the simulation. The mean values of the temperature and pressure increments are: $\delta P \sim 2$ bar, $\delta T \sim 0.05$ K while the associated time lapse is $\delta t = 800$ years (see Appendix B).

The iterations start at $P_i = 10.19^6$ kbar and $T_i = 609$ K and stop at $P_f = 12.14$ kbar and $T_f = 832$ K (point **c**, Fig. 3) which are the pressure and temperature of closure (see Discussion). At 11.72 kbar and 642 K, after 745 iterations (point **a**, Fig. 3), the garnet starts growing and its size and composition are calculated 4162 times (4907 – 745). This correspond to ~ 3.330 Ma ($4162 \times \delta t$), the time employed by the rock to cover the portion of P - T trajectory from point **a** to point **c** (Fig. 3). Over this time the garnet zoning develops, as drawn in Fig. 4a. The composition obtained suppressing volume diffusion, is drawn in Fig. 4b for a comparison. We name prograde path the portion of P - T trajectory from **a** to the pressure peak, at $P=16.09$ kbar and $T=802$ K (point **3**, Fig. 3). The highest temperature, occurring during the down-pressure path, is $T=839$ K, at $P=14.11$ kbar (thermal peak: point **4**, Fig. 3). The prograde and

TABLE 3
Self-diffusion coefficients, D° , activation energy at 1 bar, ΔE , and activation volume, ΔV , of divalent cations in garnet, used in the simulation.

	D° (cm ² /s)	ΔE (J/mol)	ΔV (cm ³ /mol)
Fe	1.3×10^{-5}	242000	5.6
Mg	1.0×10^{-3}	243040	5.3
Ca	1.7×10^{-6}	238219	6.0
Mn	5.1×10^{-4}	242276	6.0

⁵ At every iteration we minimize the Gibbs function of this system of 9 components, 22 phase components and 9 phases, under the closed system constraint dictated by the “temporary” EBC.

⁶ We are aware that fractions of kbar and K are not geologically significant. The calculation demands such precision, but the error on the estimates of P and T , depending on the model incertitude is higher, as it will be discussed.

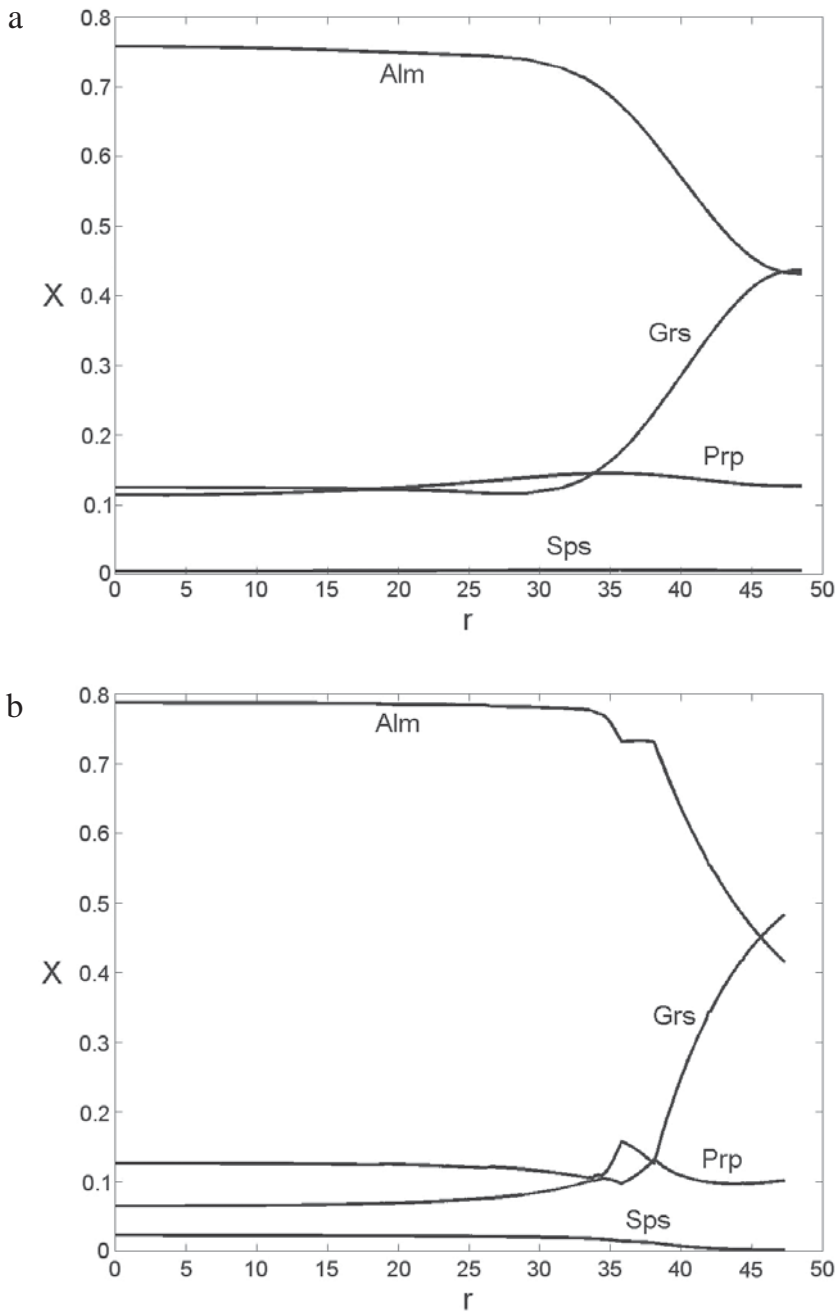


Fig. 4 – (a) Garnet zoning calculated with the segregation-dissolution model and considering volume diffusion in garnet. (b) Calculated garnet zoning considering only the segregation-dissolution model, but not volume diffusion in garnet. The comparison between the two figures stresses the smoothing role on the concentration profiles of the volume diffusion in garnet. Radius (r) is in μm .

down-pressure P - T path last, respectively, 2.042 Ma and 1.288 Ma.

The garnet nucleates when $M_g > 0$; with this condition the model introduces an overstepping of the garnet forming reactions and an induction time for nucleation. Indeed when this condition is not yet fulfilled, the garnet is already stable ($E_g > 0$), but its formation is prevented being $N_g > E_g$. This is more realistic than previous models, though semi-quantitative for the garnet surface energy is not accounted for in the Gibbs function, nor does affect the reaction rate of the garnets of smallest size. So the garnet nucleates at 11.72 kbar and 642 K (point **a**, Fig. 3) and grows with sporadic resorption episodes up to the radius of 56.2 μm (r_{max}), at 16.07 kbar and 794 K (point **b**, Fig. 3). The variation of garnet radius vs. time is plotted in Fig. 5.

Initially the garnet is nearly homogeneous; at 750 K, 15.39 kbar the concentration of grossular

increases while that of almandine decreases (see also Fig. 6); the two components have equal concentration at about 753.68 K and 15.46 kbar when the radius of garnet is 45.6 μm ; the highest concentration of grossular occurs at 759.59 K, 15.59 kbar when $r = 53.2 \mu\text{m}$. Then the zoisite becomes stable and the amount of grossular in garnet decreases, Ca being partitioned between garnet, zoisite and Ca-Tschermak in piroxene. Garnet continues to grow up to 16.07 kbar and 794 K.

The garnet growth rate is not constant (Fig. 5). The growth rate, initially high, decreases rapidly and in a continuous way until reaches the lowest value occurring at 15.39 kbar and 750 K, when the garnet radius is 38 μm at ~ 1.2 Ma. Then the rate increases and the garnet radius reaches the highest value (r_{max}), after ~ 1.9 Ma. This abrupt increase of garnet growth rate coincides with the increment of grossular in the garnet (Fig. 6b), and it is caused

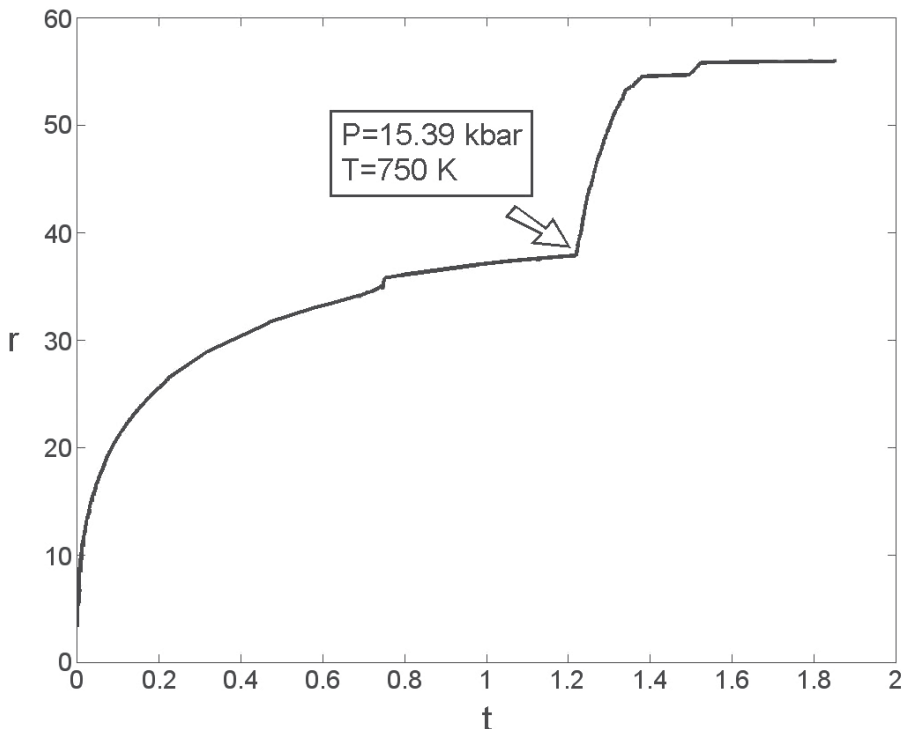


Fig. 5 – Garnet radius (μm) versus time (Ma). The garnet growth rate abruptly increases, at about 15.5 kbar and 750 K, when all the Ca released from the plagioclase makes the grossular.

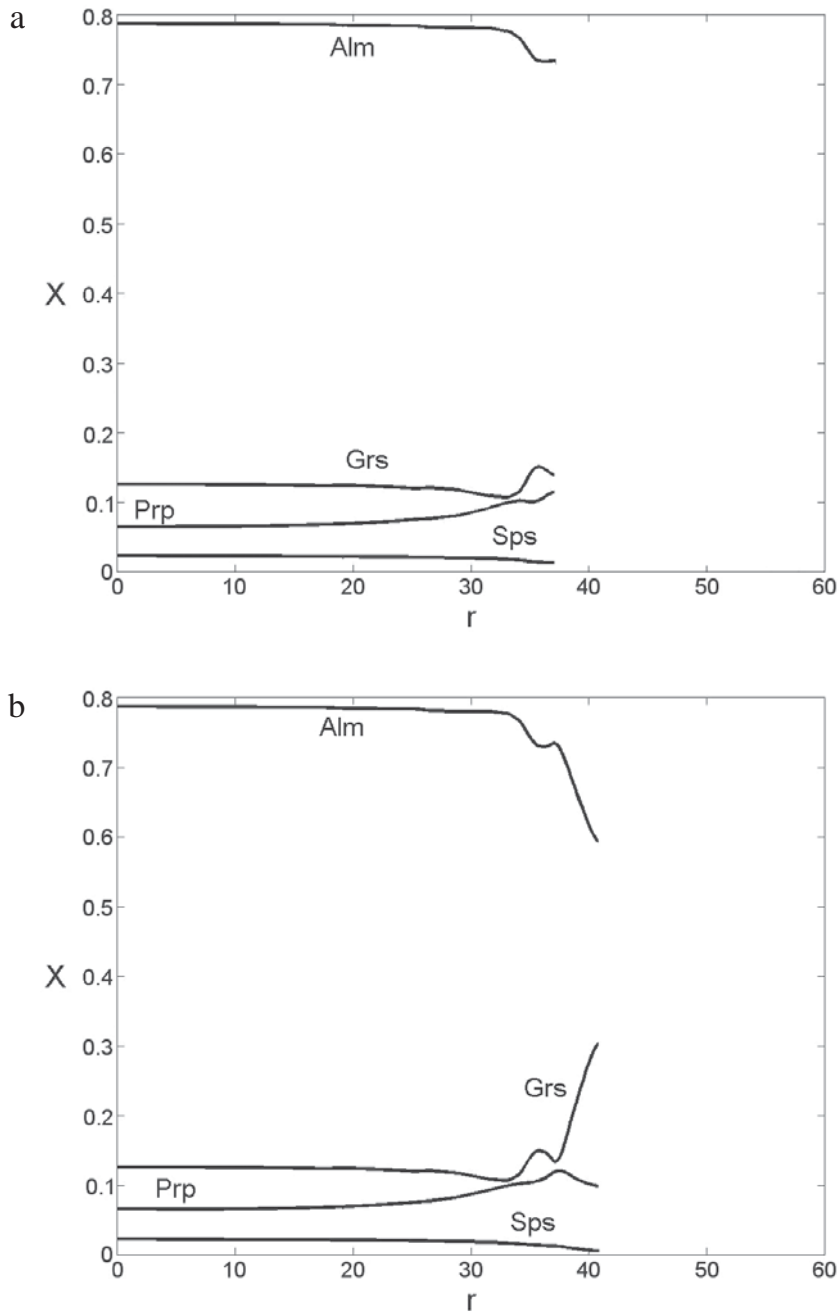
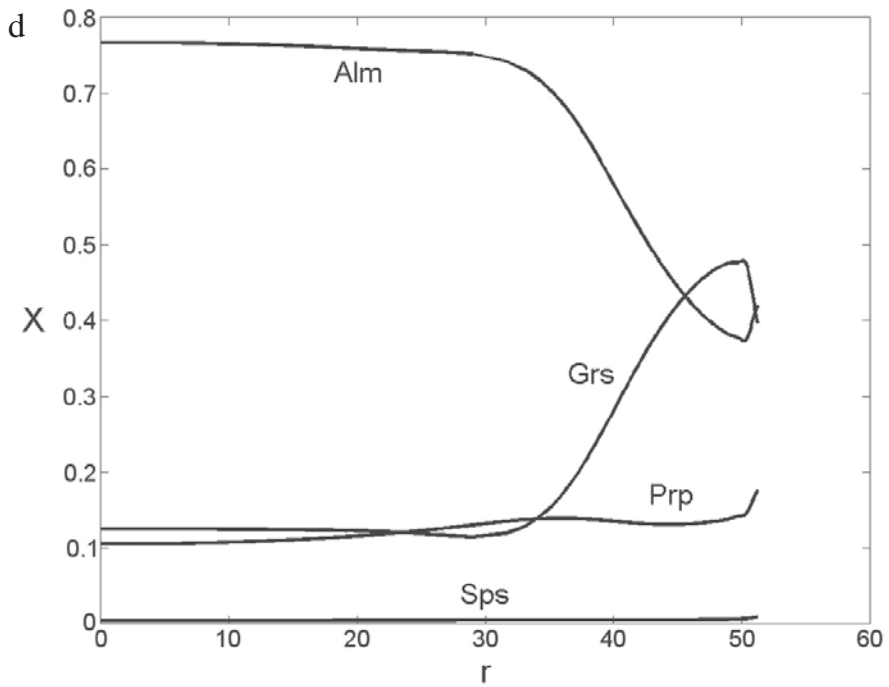
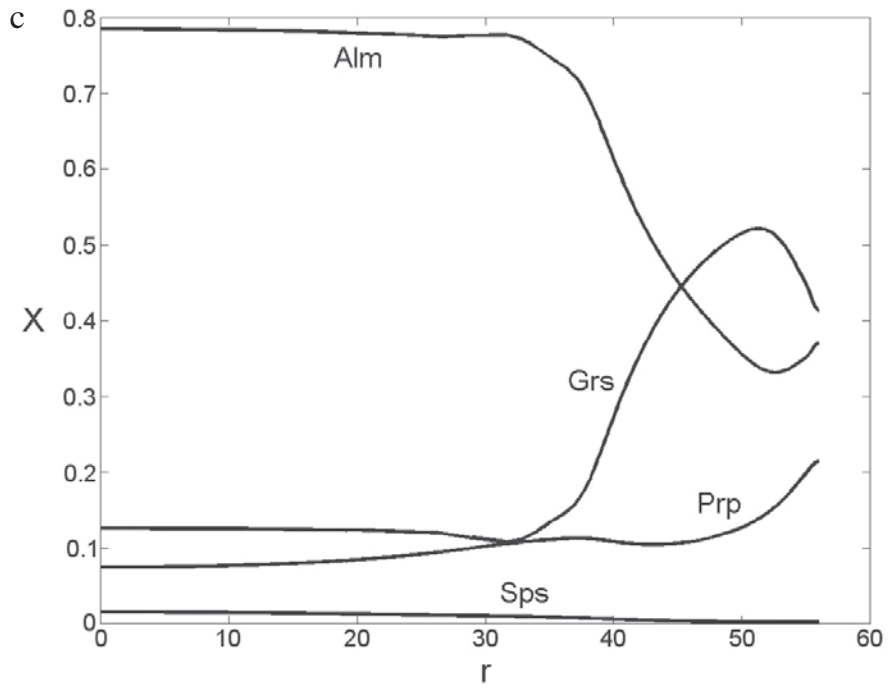


Fig. 6 – Evolution of the garnet zoning along the P - T path of Fig. 3. (a) Garnet zoning when P , T and t are 15 kbar, 735 K and ~ 1 Ma, point 1 of Fig. 3; (b) when P , T and t are 15.41 kbar, 751 K and ~ 1.21 Ma, point 2; (c) pressure peak, point 3: $P = 16.09$ kbar, $T = 802$ K and $t = 2.042$ Ma; (d) thermal peak, point 4: $P = 14.11$ kbar, $T = 839$ K, $t = 3.092$ Ma.



by the increased resorption rate of plagioclase, by the growth of Na and Ca poorer feldspars and of a jadeite-rich pyroxene.

During the decompression the dissolution of garnet proceeds in a regular way down to the radius of 48.5 μm at P_f and T_f , without abrupt variations of rate.

The Na-pyroxene becomes stable at about 12 kbar and 650 K. Its abundance slowly increases up to 15.39 kbar and 750 K; then rapidly the albite in feldspars becomes unstable forming jadeite. After the pressure peak, at about 16.05 kbar and 811 K, its abundance decreases rapidly.

The zoisite becomes stable at about 15.59 kbar and 759.69 K, and it remains stable up to the end of the P - T - t path, capturing part of the Ca released by the garnet during the down-pressure path.

The quartz abundance is determined by the balance between several net transfer reactions. It is consumed up to the peak pressure, and grows during the decompression and cooling. Phengite grows and biotite resorbs during the prograde path. With increasing pressure the mole fraction of both muscovite and eastonite end-members decreases and the proportion of Mg end-members increases; Fe is preferentially partitioned in phengite. During the decompression the net transfer reactions occur in the opposite direction.

The calculated number of moles of fluid phase (H_2O) is always nil. This implies that the reactions involving biotite, zoisite and phengite balance in such a way that the net production of water is zero. Water molecules or OH groups moved from biotite to zoisite and phengite presumably forming an intergranular adsorption layer, which could speed up also the intergranular diffusion of the elements (Ca, Mg, etc.). This same situation has also been found in a metagranodiorite of the Brossasco-Isasca Unit (Dora-Maira Massif, western Italian Alps), by Bruno *et al.* (2001).

DISCUSSION

Comparison between profiles

The measured compositional profiles are on the average well reproduced by the simulation (Fig. 4a). The main disagreement between measured and calculated zonings is observed in the garnet core. It may be caused by the igneous plagioclase zoning.

Then, it is possible that the low concentration of Ca, measured in the garnet core (Fig. 2a), was produced by the resorption, during prograde metamorphism, of a plagioclase whose rim was poor in An.

Minor differences between measured and simulated zonings are instead observed in the garnet rim, where the measured Mg molar fraction (0.06) is lower than that calculated (0.12). Observing the asymmetry of Mg concentration at the garnet rims toward the biotite and phengite, one can attribute this slight discrepancy to the coalescence of the garnets forming the corona, not considered in the simulation. The coalescence hindered the grain boundary diffusion of Mg from the garnet/biotite to the garnet/plagioclase interface. This seems to indicate that the Mg is unable to equilibrate at the scale of the coronitic structure, as well as Ca. Then, this simulation provides, indirectly, evidence of a factor of disequilibrium during garnet growth.

As stated in a previous section, when garnet grows, its calculated outer shell composition is in partitioning equilibrium with the temporary EBC; when it dissolves, during the down-pressure path, inner layers of garnet, which are out equilibrium with the temporary EBC, re-emerge. This looks sensible because the sluggishness of volume diffusion in garnet hinders the surface re-equilibration. However, because one can suppose that the surface equilibrium prevails both during growth and dissolution, we calculated diffusion profiles using Dirichlet boundary conditions, imposing partitioning equilibrium and accounting for the matter exchange between garnet and EBC. The profiles so obtained (M. Bruno, unpublished data) are similar to those calculated with the zero flow condition, in the prograde phase. Conversely in the retrograde phase, the composition at the garnet rim shows the effect of imposing equilibrium partitioning: a sharp and strong curvature reversals of the components concentration, extends inwards about 5 μm . A similar result has been described, for example, by Carlson (2002). Because, in all garnets analyzed, we do not even measure a very small curvature change near the rims, we conclude that the garnet surface was not in partitioning equilibrium during dissolution.

Fingerprints of volume diffusion

Fig. 6 shows the garnet in several moments of the P - T - t trajectory. When P , T and t are, respectively, 15 kbar, 735 K and ~ 1 Ma (point 1, Fig. 3), the garnet radius is 37.2 μm (Fig. 6a) and the volume diffusion is negligible in the low temperature segment of the trajectory.

With advancing metamorphism, at $P=15.41$ kbar, $T=751$ K and $t \sim 1.21$ Ma (point 2, Fig. 3), the garnet radius becomes 41 μm and the diffusion is still scarce (Fig. 6b).

At the peak pressure (point 3, Fig. 3) the garnet radius is 56 μm and the diffusion is evident: the garnet core is considerably enriched in Mg (compare the core composition in Fig. 6c with Fig. 6a). Afterwards, during down-pressure P - T path (from point 3, through the thermal peak 4, to c, Fig. 3), the garnet core continues to become enriched in Mg (Figs. 4a and 6d) and the Fe concentration shows an evident although milder decrease in the inner volume of garnet. Volume diffusion causes the double intersection of the concentrations of Ca and Mg.

The pressure and temperature of closure are P_f and T_f (point c in Fig. 3), because simulations performed with a longer retrograde path produced concentration profiles in disagreement with that measured at the garnet rim.

Coupling between growth and volume diffusion

The comparison between the composition shown in Fig. 4a and that calculated switching off volume diffusion in garnet, shown in Fig. 4b, as well as the comparison between the compositions of garnet at different stage of growth, drawn in Fig. 6, allows to state the following.

The volume diffusion affects the zoning in two ways: (i) directly, because it tends to homogenize the garnet, and (ii) indirectly, because resorption episodes re-introduce in the EBC elements coming from layers compositionally modified by the re-equilibration, so affecting the subsequent growth episodes. As a further consequence the inner volume of garnet records P - T - X conditions different from those of its making. In the metagranodiorite this is particularly evident during retrograde P - T - t path, when the garnet is partially resorbed, its radius decreasing by ~ 8 μm . However, such consumption does not erase the information on the final tract of

the prograde P - T - t path, because the actual garnet zoning is the result of the matter exchange, through volume diffusion, between inner layers and those that will be, but are not yet, resorbed.

Growth rate of garnet

The garnet growth rate is not continue but it abruptly increases at ~ 15.4 kbar and 750 K (Fig. 5). This is caused by the interplay of the functions N_p , N_g describing kinetics, with the functions E_p , E_g related to stability. The resulting EBC determine the stability and composition of the metamorphic phases and the peculiar profile of the Ca concentration in garnet. Such features are not expected when only grain boundary diffusion is limiting the kinetics as in the cases studied in previous works by Kretz (1974) and Carlson (1989).

We estimate that garnets, of ~ 56 μm radius, grew over periods of ~ 1.9 Ma, corresponding to an average growth rate of $\sim 9 \times 10^{-17}$ cm/s.

Petrologic implications

The MMM garnet composition can be explained in terms of the proposed clockwise P - T - t path. This is a path typical of regional metamorphism, where pressure peak ($P=16.09$ kbar, $T=802$ K, $t=2.042$ Ma) precedes the thermal peak ($P=14.11$ kbar, $T=839$ K, $t=3.092$ Ma). This result agrees with the work of Rubbo *et al.* (1999), but disagrees with previous works on Sesia Zone (Lardeaux *et al.*, 1982; Droop *et al.*, 1990; Rubatto *et al.*, 1999; Pognante, 1989, 1991), where it is supposed that maximum pressure and maximum temperatures coincide. Then, the ages estimated by Inger *et al.* (1996), Duchêne *et al.* (1997) and Rubatto *et al.* (1999) do not correspond to the maximum subduction depth, but to the thermal peak, which is about 2 kbar below the pressure peak (Fig. 3). This implies, for the maximum subduction depth an age of ~ 1 Ma older than previously estimated. Now, if we assume lithostatic pressure, a layered lithosphere composed by 20 Km thick upper crust, 10 Km thick lower crust and an upper mantle with densities of 2.7, 3.0 and 3.3 g/cm³, respectively, we can convert pressure to depth. Combining depth data with times we obtain subduction and exhumation rates of 0.75 (the value estimated by

Rubatto *et al.* (1999) is 0.7 cm/year) and 0.91 cm/year, respectively.

In conclusion this model, taking into accounts the garnet internal re-equilibration, improves the previous one (Rubbo *et al.*, 1999) extracting the information recorded by the garnet zoning and producing a qualitative richer description of the metamorphism of the granodiorite.

Approximations, estimates of parameters and errors

The largest errors on the estimate of time and by consequence of rates of garnet growth, of subduction and exhumation, depend on incertitude on input parameters, that is: the estimate of the proportion of elements in the initial EBC, the P , T conditions at the metamorphic peak, the diffusivities and thermodynamic data, and solution models. Unfortunately, the calculations involved in the zoning simulation are too complex to permit determination of uncertainties by propagation of errors. Consequently, a measure of the accuracy of the results can be obtained by varying each input parameter by an amount representing its estimated uncertainty, and reproducing again the measured zoning by adjusting the other parameters.

The whole P - T path has been translated by ± 10 K and the measured zoning has been reproduced by varying the parameters α^p and α^g by $\pm 5\%$. The duration of the metamorphic event correspondingly varied by $\pm 10\%$.

Then, the baric peak has been translated by + 2 kbar. The measured zoning has been simulated by increasing α^g by 5%, and the initial Fe/Mg ratio in the biotite, by 4%. In this case the time varied by + 15%. It has not been possible to translate the baric peak in the opposite direction. Indeed, if it is lower than 16 kbar the garnet is always grossular-poor. Therefore, we can estimate that the minimum peak pressure suffered by MMM is 16 kbar.

Calculations have also been performed by varying the initial biotite/quartz ratio in the EBC by $\pm 10\%$. Even in this case the measured concentration profile has been reproduced by modifying the parameters α , by $\pm 10\%$. The time varied of the same percentage.

In addition, calculations have been made by varying the $D^\circ(\text{Ca})$ (the less constrained by the experimental works) by $\pm 10\%$, but such

modifications did not produce significant effects on the final results. The $D^\circ(\text{Ca})$ used in this work agrees quite well with the value proposed by Carlson (2006) for almandine garnet ($1.57 \times 10^{-6} \text{ cm}^2 \text{ s}^{-1}$)

Finally, we assumed that the garnet corona is a prism that grows only in the direction perpendicular to the original contact between biotite and plagioclase. We also assumed a planar growth front having constant area of $500 \times 500 \mu\text{m}^2$.

The concentration profiles obtained in the simulation are similar to those calculated for spherical garnet during the prograde path, but they are stretched in the direction of growth and show shallow gradients. The size of the garnet in the growth direction is so increased that volume diffusion does not modify significantly the bulk composition and the calculated garnet composition do not converge to the measured one. We attempted to improve convergence modifying the functions N_p , N_g and the P - T - t trajectory, without success.

It is clear that the empirical functions (2) and (3) lumps together reaction and transport processes whose properties are unknown; so such functions depend on parameters not related to well identified kinetic step. The parameters of the P - T path, the composition of the granodiorite and the diffusion coefficients are better constrained; varying them within reasonable limits and adjusting the remaining parameters we have estimated an upper and lower error of + 15% and - 10%, on the metamorphic event duration.

It is a support to our estimate of the duration of MMM metamorphism the agreement with the independent radiometric determination (Rubatto *et al.*, 1999).

Notwithstanding the difficulties encountered when trying to describe the kinetic of metamorphic reactions, we maintain that this work and simulation works in general are useful to addresses some complexities involved in the analyses of non equilibrium assemblages and indicates and warns against some possible misinterpretations.

ACKNOWLEDGEMENT

We are grateful to Professor R. Compagnoni for useful discussions and encouragement and to Professor W. D. Carlson for the comments to a previous version of the manuscript. We are grateful to

Professors B. Cesare and L. Gaggero: their criticism and suggestions improved the quality of this work.

REFERENCES

- ANDERSON D.E. and OLIMPIO J.C. (1977) – *Progressive homogenization of metamorphic garnets, south Molnar, Scotland: Evidence for volume diffusion*. *Can. Mineral.* **15**, 205-216.
- BRUNO M. (2002a) – *Granato: un nuovo modello di crescita. Dalla cinetica alla ricostruzione della traiettoria P-T-t*. PhD Thesis (in Italian), University of Turin.
- BRUNO M. (2002b) – *Garnet: a new growth model. From kinetic to reconstruction of the P-T-t path*. *Plinius* **27**, 57-61.
- BRUNO M., COMPAGNONI R. and RUBBO M. (2001) – *The ultra-high pressure coronitic and pseudomorphous reactions in a metagranodiorite from the Brossasco-Isasca Unit, Dora-Maira Massif, western Italian Alps: a petrographic study and equilibrium thermodynamic modelling*. *J. Metamorph. Geol.* **19**, 33-43.
- CARLSON W.D. (1989) – *The significance of intergranular diffusion to the mechanisms and kinetics of porphyroblast crystallization*. *Contrib. Mineral. Petrol.* **103**, 1-24.
- CARLSON W.D. (2002) – *Scales of disequilibrium and rates of equilibration during metamorphism*. *Am. Mineral.* **87**, 185-204.
- CARLSON W.D. (2006) – *Rates of Fe, Mg, Mn, and Ca diffusion in garnet*. *Am. Mineral.* **91**, 1-11.
- CHAKRABORTY S. and GANGULY J. (1991) – *Compositional zoning and cation diffusion in garnets*. In: GANGULY J. (ed.), *Diffusion, atomic ordering, and mass transport*, *Adv. Phys. Geochim.* **8**. Springer-Verlag, Berlin, 120-175.
- CHAKRABORTY S. and GANGULY J. (1992) – *Cation diffusion in aluminosilicate garnets: Experimental determination in spessartine-almandine diffusion couples, evaluation of effective binary diffusion coefficients, and applications*. *Contrib. Mineral. Petrol.* **111**, 74-86.
- CHERNOFF C.B. and CARLSON W.D. (1997) – *Disequilibrium for Ca during growth of politic garnet*. *J. Metamorph. Geol.* **15**, 421-438.
- COMPAGNONI R. (1977) – *The Sesia-Lanzo Zone: high pressure-low temperature metamorphism in the Austroalpine continental margin*. *Rend. Soc. It. Min. Petr.* **33**, 335-374.
- COMPAGNONI R., DAL PIAZ G.V., HUNZIKER J.C., GOSSO G., LOMBARDO B. and WILLIAMS P.F. (1977) – *The Sesia-Lanzo Zone, a slice of continental crust with Alpine high-pressure-low temperature assemblages in the western Italian Alps*. *Rend. Soc. It. Min. Petr.* **33**, 281-334.
- COMPAGNONI R., HIRAJIMA T. and CHOPIN C. (1995) – *Ultra-high-pressure metamorphic rocks in the Western Alps*. In: COLEMAN R.G. and WANG X. (eds.), *Ultra-high-pressure metamorphism*. Cambridge University Press, Cambridge, 206-243.
- COMPAGNONI R. and MAFFEO B. (1973) – *Jadeite-bearing metagranites l. s. and related rocks in the Mount Mucrone area (Sesia-Lanzo Zone, Western Italian Alps)*. *Schweiz. Mineral. Petrogr. Mitt.* **53**, 355-378.
- DAL PIAZ G.V., HUNZIKER J.C. and MARTINOTTI G. (1972) – *La zona Sesia-Lanzo e l'evoluzione tettonico-metamorfica delle Alpi Nord-occidentali interne*. *Mem. Soc. Geol. It.* **11**, 433-466.
- DEMPSTER T.J. (1985) – *Garnet zoning and metamorphism of the Barrovian Type area, Scotland*. *Contrib. Mineral. Petrol.* **89**, 30-38.
- DROOP G.T.R., LOMBARDO B. and POGNANTE U. (1990) – *Formation and distribution of eclogite facies rocks in the Alps*. In: CARSWELL D.A. (ed.), *Eclogite facies rocks*. Blackie, Glasgow, 225-259.
- DUCHÈNE S., BLICHERT T.J., LUISS B., TÉLOUK P., LARDEAUX J.M. and ALBARÈDE F. (1997) – *The Lu-Hf dating of garnets and the ages of the Alpine high-pressure metamorphism*. *Nature* **387**, 586-589.
- FLORENCE F.P. and SPEAR F.S. (1991) – *Effects of diffusional modification of garnet growth zoning on P-T path calculations*. *Contrib. Mineral. Petrol.* **107**, 487-500.
- FLORENCE F.P. and SPEAR F.S. (1993) – *Influences of reaction history and chemical diffusion on P-T calculations for staurolite schists from the Littleton Formation, northwestern New Hampshire*. *Am. Mineral.* **78**, 345-359.
- FUHRMAN M. and LINDSLEY D.H. (1988) – *Ternary-feldspar modeling and thermometry*. *Am. Mineral.* **73**, 201-215.
- GANGULY J., CHENG W. and CHAKRABORTY S. (1998) – *Cation diffusion in aluminosilicate garnets: experimental determination in pyrope-almandine diffusion couple*. *Contrib. Mineral. Petrol.* **131**, 171-180.
- GANGULY J., CHENG W. and TIRONE M. (1996) – *Thermodynamics of aluminosilicate garnets solid solution: new experimental data, and optimized model, and thermometric applications*. *Contrib. Mineral. Petrol.* **126**, 137-151.

- HIRSCH D.M., PRIOR D.J. and CARLSON W.D. (2003) – *An overgrowth model to explain multiple, dispersed high-Mn regions in the cores of garnet porphyroblasts*. *Am. Mineral.* **88**, 131-141.
- HOLLAND T.J.B. and POWELL R. (1990) – *An enlarged and updated internally consistent thermodynamic dataset with uncertainties and correlation: the system K_2O - Na_2O - CaO - MgO - FeO - Fe_2O_3 - Al_2O_3 - TiO_2 - SiO_2 - C - H_2 - O_2* . *J. Metamorph. Geol.* **8**, 89-124.
- INGER S., RAMSBOTHAM W., CLIFF R.A. and REX D.C. (1996) – *Metamorphic evolution of the Sesia-Lanzo Zone, Western Alps: time constraints from multi-system geochronology*. *Contrib. Mineral. Petrol.* **126**, 152-168.
- KOHN M.J., ORANGE D.L., SPEAR F.S., RUMBLE III D. and HARRISON T.M. (1992) – *Pressure, temperature, and structural evolution of west-central New Hampshire: Hot thrusts over cold basement*. *J. Petrol.* **33**, 521-556.
- KONRAD-SCHMOLKE M., HANDY M.R., BABIST J. and O'BRIEN P.J. (2005) – *Thermodynamic modelling of diffusion-controlled garnet growth*. *Contrib. Mineral. Petrol.* **16**, 181-195.
- KOONS P.O. (1982) – *An investigation of experimental and natural high pressure assemblages from the Sesia Zone, western Alps, Italy*. PhD Thesis, ETH Zurich.
- KOONS P.O., RUBIE D.C. and FRUEH-GREEN G. (1987) – *The effects of disequilibrium and deformation on the mineralogical evolution of quartz-diorite during metamorphism in the eclogite facies*. *J. Petrol.* **28**, 679-700.
- KRETZ R. (1974) – *Some models for the rate of crystallization of garnet in metamorphic rocks*. *Lithos* **7**, 123-131.
- KRETZ R. (1983) – *Symbols for rock-forming minerals*. *Am. Mineral.* **68**, 277-279.
- LANG H.M. (1996) – *Pressure-temperature-reaction history of metapelitic rocks from the Maryland Piedmont on the basis of correlated garnet zoning and plagioclase-inclusion composition*. *Am. Mineral.* **81**, 1460-1475.
- LARDEAUX J.M., GOSSO G., KIENAST J.R. and LOMBARDO B. (1982) – *Relations entre le métamorphisme et la déformation dans la Zone Sesia-Lanzo (Alpes Italiennes)*. *Bull. Soc. Géol. France* **24**, 793-800.
- LASAGA A.C. (1979) – *Multicomponent exchange and diffusion in silicates*. *Geochim. Cosmochim. Acta* **43**, 455-469.
- LOOMIS T.P. (1978a) – *Multicomponent diffusion in garnet: I. Formulation of isothermal models*. *Am. J. Sci.* **278**, 1099-1118.
- LOOMIS T.P. (1978b) – *Multicomponent diffusion in garnet: II. Comparison of models with natural data*. *Am. J. Sci.* **278**, 1119-1137.
- LOOMIS T.P. (1981) – *An investigation of disequilibrium growth processes of plagioclase in the system anorthite-albite-water by methods of numerical simulation*. *Contrib. Mineral. Petrol.* **76**, 196-205.
- LOOMIS T.P. (1983) – *Compositional zoning of crystals: a record of growth and reaction history*. In: SAXENA S.K. (ed.), *Kinetics and equilibrium in mineral reactions*. Springer-Verlag, Berlin, 1-60.
- MARMO B.A., CLARKE G.L. and POWELL R. (2002) – *Fractionation of bulk rock composition due to porphyroblast growth: effects on eclogite facies mineral equilibria, Pam Peninsula, New Caledonia*. *J. Metamorph. Geol.* **20**, 151-165.
- OBERHÄNSLI R., HUNZIKER J.C., MARTINOTTI G. and STERN W.B. (1985) – *Geochemistry, geochronology and petrology of Monte Mucrone: an example of eo-Alpine eclogitization of Permian granitoids in the Sesia-Lanzo Zone, Western Alps, Italy*. *Chem. Geol.* **52**, 165-184.
- OKUDAIRA T. (1996) – *Temperature-time path for the low-pressure Ryoke metamorphism, Japan, based on chemical zoning in garnet*. *J. Metamorph. Geol.* **14**, 427-440.
- ONGE S.M.R. (1987) – *Zones poikiloblastic garnets: P-T paths and syn-metamorphic uplift through 30 km of structural depth, Wopmay Orogen, Canada*. *J. Petrol.* **28**, 1-21.
- POGNANTE U. (1989) – *Lawsonite, blueschist and eclogite formation in the southern Sesia Zone (western Alps, Italy)*. *Eur. J. Mineral.* **1**, 89-104.
- POGNANTE U. (1991) – *Petrological constraints on the eclogite and blueschist-facies metamorphism and P-T-t paths in the Western Alps*. *J. Metamorph. Geol.* **9**, 5-17.
- POWELL R. (1978) – *Equilibrium Thermodynamics in Petrology. An Introduction*. Harper and Row, London.
- RUBATTO D., GEBAUER D. and COMPAGNONI R. (1999) – *Dating of eclogite-facies zircons: the age of Alpine metamorphism in the Sesia-Lanzo Zone (Western Alps)*. *Earth Planet. Sci. Lett.* **167**, 141-158.
- RUBBO M., BORGHI A. and COMPAGNONI R. (1999) – *Thermodynamic analysis of garnet growth zoning in eclogitised granodiorite from M. Mucrone, Sesia*

- Zone, Western Alps. *Contrib. Mineral. Petrol.* **137**, 289-303.
- SELVERSTONE J. and SPEAR F.S. (1985) – *Metamorphic P-T paths from pelitic schists and greenstones in the southwest Tauern Window, eastern Alps*. *J. Metamorph. Geol.* **3**, 439-465.
- SELVERSTONE J., SPEAR F.S., FRANZ G. and MORTEANI G. (1984) – *High pressure metamorphism in the SW Tauern window, Austria: P-T paths from hornblende-kyanite-staurolite schists*. *J. Petrol.* **25**, 501-531.
- SPEAR F.S. (1988a) – *The Gibbs method and Duhem's theorem: the quantitative relationships among P, T, chemical potential, phase composition and reaction progress in igneous and metamorphic systems*. *Contrib. Mineral. Petrol.* **99**, 249-256.
- SPEAR F.S. (1988b) – *Metamorphic fractional crystallization and internal metasomatism by diffusional homogenization of zoned garnets*. *Contrib. Mineral. Petrol.* **99**, 507-517.
- SPEAR F.S. (1993) – *Metamorphic Phase Equilibria and Pressure-Temperature-Time Paths*. Mineralogical Society of America, Washington, DC.
- SPEAR F.S., KOHN M.J., FLORENCE F.P. and MENARD T. (1991) – *A model for garnet and plagioclase growth in pelitic schists: implications for thermobarometry and P-T path determinations*. *J. Metamorph. Geol.* **8**, 683-696.
- SPEAR F.S. and RUMBLE III D. (1986) – *Pressure, temperature and structural evolution of the Orfordville Belt, west central New Hampshire*. *J. Petrol.* **27**, 1071-1093.
- SPEAR F.S. and DANIEL C.G. (2001) – *Diffusion control of garnet growth, Harpswell Neck, Maine, USA*. *J. Metamorph. Geol.* **19**, 179-195.
- STÜWE K. (1997) – *Effective bulk composition changes due to cooling: a model predicting complexities in retrograde reaction textures*. *Contrib. Mineral. Petrol.* **129**, 43-52.
- TRACY R.J., ROBINSON P. and THOMPSON A.B. (1976) – *Garnet composition and zoning in the determination of temperature and pressure of metamorphism, central Massachusetts*. *Am. Mineral.* **61**, 762-775.
- TROPPEP P. and ESSENE E.J. (2002) – *Thermobarometry in eclogites with multiple stages of mineral growth: an example from the Sesia-Lanzo Zone (Western Alps, Italy)*. *Schweiz. Mineral. Petrogr. Mitt.* **82**, 487-514.
- VANCE D. and HOLLAND T.J.B. (1993) – *Detailed isotopic and petrological study of a single garnet from the Gassetts Schist, Vermont*. *Contrib. Mineral. Petrol.* **114**, 101-118.
- WOODSWORTH G.J. (1977) – *Homogenization of zoned garnets from pelitic schists*. *Can. Mineral.* **15**, 230-242.
- YARDLEY B.W.D. (1977) – *An empirical study of diffusion in garnet*. *Am. Mineral.* **62**, 793-800.
- ZUCALI M., SPALLA M.I. and GOSSO G. (2002) – *Fabric evolution and reaction rate as correlation tool: the example of the Eclogiti Micaschists complex in the Sesia-Lanzo Zone (Monte Mucrone – Monte Mars, Western Alps, Italy)*. *Schweiz. Mineral. Petrogr. Mitt.* **82**, 429-454.

APPENDIX A

The equilibrium calculations are performed at every iteration k by minimizing, at constant pressure (P_k), temperature (T_k) and bulk composition (EBC at the iteration k), the Lagrangian:

$$L(\mathbf{n}, \lambda) = G - \lambda (\mathbf{A}\mathbf{n} - \mathbf{b}) \quad (\text{A1})$$

G is the Gibbs function:

$$G(T, P, \mathbf{n}) = \sum \mu_i n_i; \quad \mathbf{n}^T = [n_p, \dots, n_p, \dots, n_m] \quad (\text{A2})$$

$\mathbf{A}(l, m)$ is the formula matrix, l the number of system components, m the number of phase components, $\mathbf{b}(l)$ the element abundance vector, $\lambda(l)$ the row vector of Lagrange multipliers, μ_i the chemical potentials of end members of each phase at P_k and T_k , n_i their mole numbers which are constrained by the mass balance equation ($\mathbf{A}\mathbf{n} - \mathbf{b} = 0$) and non-negativity conditions ($n_i \geq 0$). In a cumbersome notation the sum in (A2) should be replaced by $\sum_{\alpha} \sum_j \mu_j^{\alpha} n_j^{\alpha}$, where α runs over the phases and j over the phases components.

APPENDIX B

The program GARGROW is written in Fortran 90. The program uses NAG commercial routines to numerically minimize the Gibbs function and to integrate the diffusion equation. Routines calculating volume diffusion can be switched on or off, thus the user can choose whether or not to consider the volume diffusion in garnet when modeling the zoning. We performed a sequence of calculations, increasing progressively the number of subdivision of the P - T path (greater iteration number and lower re-equilibration time), until a further increase of the number of subdivisions, corresponding to smaller and smaller δP , δT and δt steps, did not produce variations in the results.

GARGROW does not effect all the minimizations initially planned; the proportion of the failed ones, increases somewhat as the subdivision becomes finer. The results reported in the section "model application", correspond to 4907 successful minimizations, in turn corresponding to the steps $\delta P \sim 2$ bar, $\delta T \sim 0.05$ K and $\delta t = 800$ years, over a total minimization attempts of 9500. We estimate that these failures do not affect the calculated garnet zoning, but introduce some inaccuracies in the calculated instantaneous garnet growth rate for the failures are not homogeneously distributed.